Chinese Physics B

Epitaxial fabrication of monolayer cupper arsenide on Cu(111)

To cite this article before publication: Shuai Zhang *et al* 2020 *Chinese Phys. B* in press https://doi.org/10.1088/1674-1056/ab8db3

Epitaxial fabrication of monolayer cupper arsenide on Cu(111) *

Shuai Zhang(张帅)[1], Yang Song(宋洋)[1], Jin Mei Li(李金梅)[2], Zhenyu Wang(王振宇)[1], Chen Liu(刘晨)[2], Jia Ou Wang(王嘉鸥)[2], Lei Gao(高蕾)[3], Jian-Chen Lu(卢建臣)[3], Yu Yang Zhang(张余洋)[1,4], Xiao Lin(林晓)[1,4,‡],Jinbo Pan(潘金波)[1,†], Shi Xuan Du(杜世萱)[1,4], and Hong-Jun Gao(高鸿钧)[1,4,§]

[1]*Institute of Physics & University of Chinese Academy of Sciences, Chinese Academy of Sciences, Beijing 100190, China*
[2]*Institute of High Energy Physics, Chinese Academy of Sciences, Beijing 100190, China*
[3] *Kunming University of Science and Technology, Kunming 650500, China*
[4]*CAS Center for Excellence in Topological Quantum Computation, University of Chinese Academy of Sciences, Beijing 100190, China*

Here, we report the epitaxial growth of monolayer cupper arsenide (CuAs) with a honeycomb lattice on Cu(111) by molecular beam epitaxy (MBE). Scanning tunneling microscopy (STM), low energy electron diffraction (LEED), X-ray photoelectron spectroscopy (XPS) and density functional theory (DFT) verify the $\sqrt{3}\times\sqrt{3}$ superlattice of monolayer CuAs on Cu(111) substrate. Angle-resolved photoemission spectroscopy (ARPES) measurements together with DFT calculations demonstrate the electronic band structures of monolayer CuAs and reveal its metallic nature. Further calculations show that charge transfer from Cu(111) substrate to monolayer CuAs lift the Fermi level and tune the band structure of monolayer CuAs. This high-quality epitaxial monolayer CuAs with potential tunable band gap hold promise on the applications in nano-electronic devices.

Keywords: cupper arsenide (CuAs), band structure, scanning tunneling microscopy (STM)

PACS: 73.20.At, 81.15.-z, 82.20.Wt

* Project supported by the National Key Research & Development Program of China (Grant Nos. 2016YFA0202300 and 2018YFA0305800), the National Natural Science Foundation of China (Grant Nos. 61888102, 11604373, 61622116, and 51872284), the Strategic Priority Research Program of Chinese Academy of Sciences (Grant Nos. XDB30000000 and XDB28000000), and the University of Chinese Academy of Sciences. A portion of the research was performed in the CAS Key Laboratory of Vacuum Physics.
‡ Corresponding author. E-mail: xlin@ucas.ac.cn
† Corresponding author. E-mail: jbpan@iphy.ac.cn
§ Corresponding author. E-mail: hjgao@iphy.ac.cn

1. Introduction

The discovery of graphene[1-3] opens a door of two dimensional (2D) materials, bringing plenty of possibilities in material world. The extreme thickness of 2D materials limits the motion of electrons, resulting in quite different properties from their bulk counterpart. For example, graphene is transparent[4] while graphite is not. Based on novel properties, 2D materials hold great potentials in industrial applications.[5-8] The exotic properties of 2D materials originate from diverse degrees of freedom, including the combinations of distinctive elements, different phases, and stacked orders. 2D materials could be composed of single-element or several elements, the former such as graphene,[9] silicene,[10] germanene,[11] borophene,[12] stanene,[13] the latter including transition metal chalcogenides,[14, 15] oxides[16, 17], and so on. Phase also influences the physical properties dramatically. For instance, 2H-WSe_2 is a semiconductor[18] while 1T'-WSe_2 demonstrate a metallic nature with enhanced electrocatalytic activity.[19] Compared with bulk, 2D materials intrinsically feature the multiformity of stacking order. As was reported previously, CrI_3 displays layer-dependent magnetism, from ferromagnetic in monolayer, to antiferromagnetic in bilayer, and back to ferromagnetic in trilayer and bulk.[20, 21]

However, compared with 2D material with layered bulk counterpart, the research of 2D material without layered bulk counterpart is rarely reported. Recently, monolayer Cu_2Se and CuSe were experimentally synthesized and exhibited adjustable properties, whose bulk counterparts were nonlayered.[22, 23] Cu_2Se on bilayer graphene displays a purely thermal structural phase transition at 147 K.[22] Grown on Cu(111), CuAs was endowed with moiré patterns or nanopores due to lattice mismatch between CuSe and Cu substrate.[23, 24] Besides, the property of CuSe is flexible, ranging from semiconductor to metal with Dirac nodal line fermions (DNLFs).[24] These findings offer a route to explore new 2D materials with novel properties.

Here, we report the epitaxial growth of flat monolayer CuAs endowed with a honeycomb lattice on a Cu(111) substrate by molecular beam epitaxy (MBE). By

combining characterizations of scanning tunneling microscopy (STM), low-energy electron diffraction (LEED), X-ray photoelectron spectroscopy (XPS) and first-principles calculations, we confirmed the atomic structures and $\sqrt{3} \times \sqrt{3}$ superstructures of monolayer CuAs on the Cu(111) substrate. Angle-resolved photoemission spectroscopy (ARPES) measurements revealed the band structure of monolayer CuAs on the Cu(111), which is further confirmed by DFT calculations. Further calculations show that the Fermi level of free-standing monolayer CuAs will be lift approximately 2.0 eV when the monolayer CuAs is put onto the Cu(111) substrate.

2. **Methods**

Sample preparations and characterizations Experiments were performed in an ultra-high vacuum (UHV) LT-STM system (Omicron), with a base pressure better than 1×10^{-9} mbar, equipped with a standard MBE capability and a LEED facility, and a low temperature STM (4.2 K and 77 K). Cu(111) substrate was cleaned by several cycles of Ar^+ ion sputtering and annealing. The cleanness of Cu(111) surface was checked by STM. High-purity arsenic atoms from a Knudsen diffusion cell were evaporated onto the cupper substrate kept at 470 K. After deposition, the sample was subsequently annealed at 470 K for 1 hour to achieve arsenication and crystallization. Finally, the sample was cooled down to room temperature at a rate of 3 K/min. LEED and STM measurements were carried out in the same UHV chamber. STM images were acquired in the constant-current mode at 4.2 K, by using an electrochemically etched tungsten tip. The bias voltage is defined as the sample bias with respect to the tip. The Nanotec Electronica WSxM software was used to process the STM images. The sample was transferred by a UHV transfer suitcase to another UHV chamber equipped with XPS and ARPES facilities without breaking the UHV conditions. XPS and ARPES results were acquired at room temperature.

First-principles calculations Density functional theory (DFT) calculations were performed using the projector augmented wave (PAW) method with the local density approximation (LDA) functional,[25] which is implemented in the Vienna Ab initio Simulation Package (VASP) code.[26, 27] The rotationally invariant LDA+U formalism proposed is used and U_{eff} is chosen as 6.52 eV for Cu.[28, 29] The spin-orbit coupling (SOC) effect is included in calculations of band structures. The electron wavefunctions are expanded in plane wave basis with a kinetic energy cutoff of 450 eV. A vacuum layer of ~15 Å was applied. A slab model of 1×1 monolayer CuAs on $\sqrt{3}\times\sqrt{3}$ ten-layered Cu(111) is used to investigate the electronic properties of CuAs monolayer on copper substrate. The size of the unit cell is 4.23 Å × 4.23 Å. The atoms in CuAs layer and top three Cu layers are fully relaxed until the residual forces on each atom are smaller than 0.02 eV $Å^{-1}$. The k-points sampling is 21 × 21 × 1.

3. Results and discussion

Monolayer CuAs films were grown by a straightforward arsenication of a Cu(111) substrate. Arsenic atoms were deposited onto a Cu(111) substrate kept at 470 K, and then the sample was annealed at 470 K to obtain an epitaxial monolayer CuAs film. A typical LEED pattern of as-grown monolayer CuAs on Cu(111) substrate was obtained after growth, as shown in Figures 1(a). The LEED pattern is composed of Cu(111) diffraction spots as well as unambiguous $\sqrt{3}\times\sqrt{3}$ structures, which indicates a lattice constant of 0.443 nm for the monolayer CuAs. Figure 1(b) is a 200 $\times$200 nm^2 STM image of monolayer CuAs, showing overall fluctuations of the sample. No higher structure could be found except clear steps, indicating the growth mode is layer by layer. In order to verify the chemical compositions of the sample, we performed XPS measurements. Figure 1(c) is a typical As 3d spectrum, endowed with two prominent peaks at 41.06 eV (As $3d_{5/2}$) and 41.69 eV (As $3d_{3/2}$). The position of two As $3d_{5/2}$ peaks for our sample locate between elemental As (41.62 eV)[30] and GaAs (40.9 eV)[31], indicating that the chemical state of As in the sample is minus. In

addition, a typical XPS spectrum for Cu depicts a peak located at 932.4 eV, as shown in Figure 1(d), which corresponds to Cu $2p_{3/2}$ and is slightly shifted from elemental Cu. The XPS results demonstrate that our sample is full crystallization and complete formation of monolayer CuAs on Cu(111) substrate.

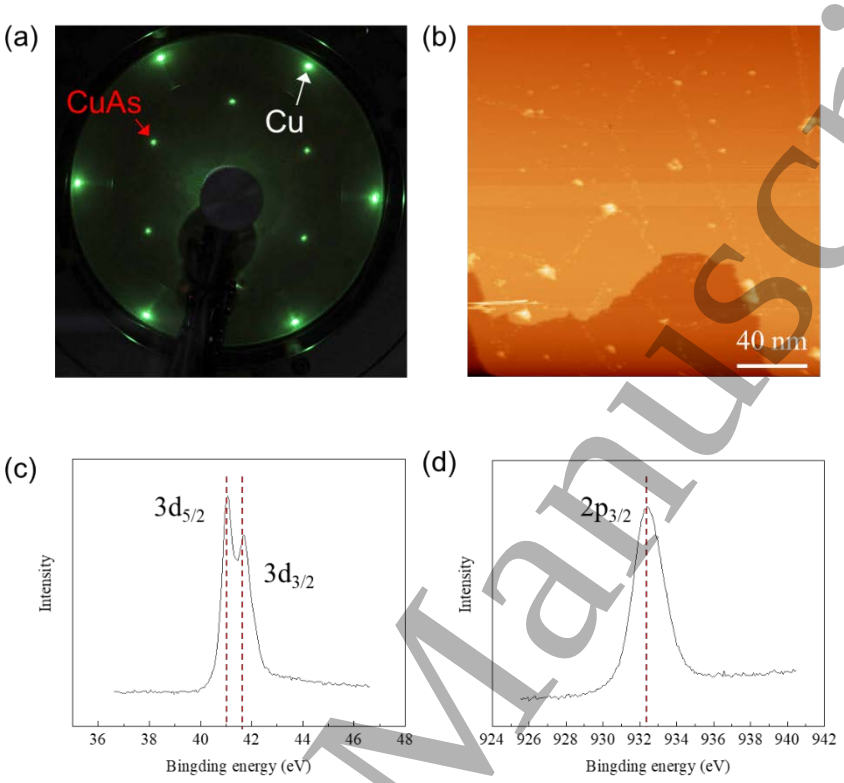

Fig. 1. STM, LEED and XPS spectra of monolayer CuAs on a Cu(111) substrate. (a) LEED pattern of CuAs on Cu(111). White arrow denotes patterns from Cu(111), and red arrow denotes the diffraction spots of CuAs. (b) Large-area STM image of CuAs. ($I = 0.05$ *nA*, $V_b = -1$ *V*) (c) High-resolution XPS spectrum for As 3d. Two prominent peaks locate at 41.06 eV (As $3d_{5/2}$) and 41.69 eV (As $3d_{3/2}$). (d) XPS spectrum from the core level of Cu 2p. The peak at 932.4 eV indicative of Cu $2p_{3/2}$.

To investigate the atomic structure of the monolayer CuAs, we performed a STM characterization. Figure 2(a) is a typical STM image of monolayer CuAs, showing a very flat terrace except some bright protrusions. Careful observations reveal that the protuberances are chain structure. According to the experience of selenium atoms on metal substrate, [32] we attribute the protrusions to extra arsenic atoms on monolayer CuAs. By constant height STM mode, atomic resolution STM image was achieved in Figure 2(b). From which, uniform honeycomb lattice could be resolved. The lattice

constant is measured 0.43 ± 0.02 nm, perfectly consistent with LEED results.

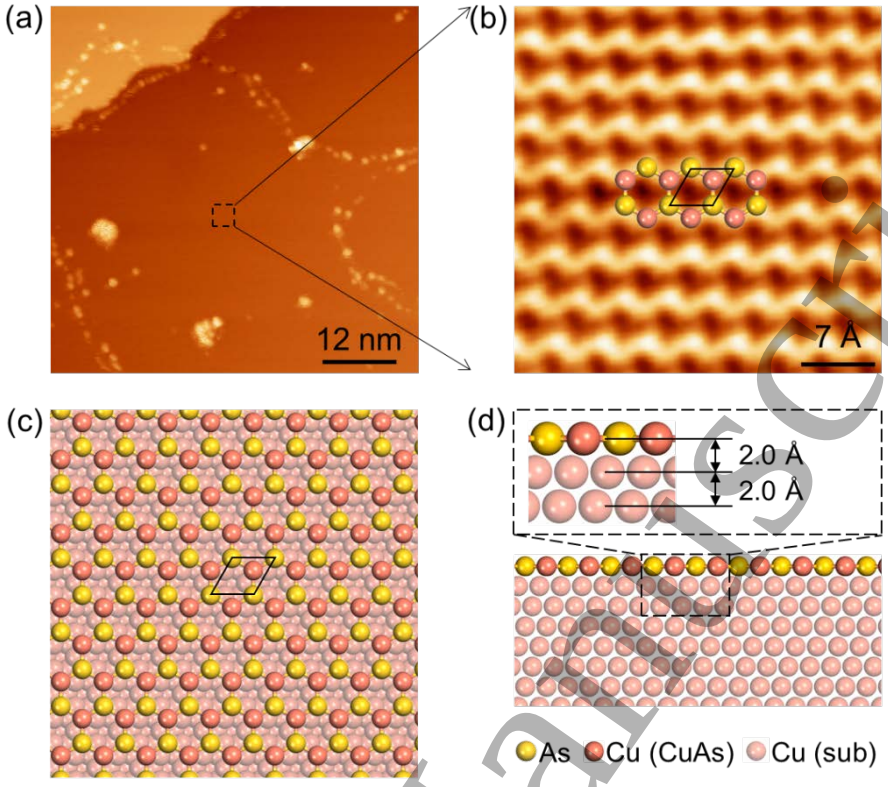

Fig. 2. Atomic structure of CuAs. (a) Close-up STM image of monolayer CuAs. The bright protuberances are extra As atoms. (*I = 0.05 nA, V_b = −1 V*) (b) Atomic resolution STM image of CuAs, clearly showing the honeycomb lattice. The black rhombus denotes a unit cell. (*I = 5 nA, V_b = −20 mV*) (c) Fully-relaxed atomic model of CuAs on Cu(111) substrate, depicting $\sqrt{3} \times \sqrt{3}$ superstructure. The black rhombus denotes a unit cell. (d) Side view of CuAs, showing the planner structure.

In order to get a better understanding of the atomic structure of the CuAs layer, we perform DFT calculations and propose a planar honeycomb structure of CuAs as shown in Figure 2(c) and (d). Arsenic atoms and cupper atoms of CuAs are lying on the fcc sites of the Cu(111) surface and forming a honeycomb structure, which makes up a $(\sqrt{3} \times \sqrt{3})R30°$ superstructure on Cu(111) substrate. However, different from CuSe[24] and ZnO,[33] we do not observe moiré patterns at CuAs/Cu(111) sample by STM and LEED, which indicates that the monolayer CuAs match well with the Cu(111) substrate.

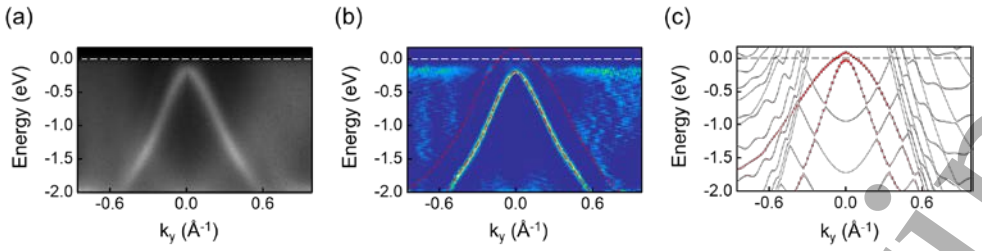

Fig. 3. ARPES data and DFT calculated band structure of monolayer CuAs on Cu(111) substrate. (a) Energy-momentum dispersion along M-Γ-K directions in the hexagonal Brillouin zone. (b) Second-derivative spectrum of the raw ARPES data in (a). The overlaid lines mark the two bands. (c) First principle calculated band structure for monolayer CuAs on Cu(111).

Electronic structure of monolayer CuAs was investigated by ARPES and DFT. Figure 3(a) displays ARPES data measured along the high symmetry direction M-Γ-K. We find that there was one hole-like band around the Fermi level. Second-derivative ARPES spectrum of raw experimental band structures (Figure 3a) are depicted in Figure 3(b) to enhance the visibility of the hole-like bands. Second-derivative ARPES spectra agrees well with theory results. Here, two hole-like bands marked by red lines emerge, and the upper band cross the Fermi level, indicating a metallic nature of monolayer CuAs on Cu(111) substrate. To attain more electronic band details, we performed DFT calculations. The calculated band structure is depicted in Fig. 3(c). A direct comparison between the ARPES data and calculated band structure shows an excellent agreement.

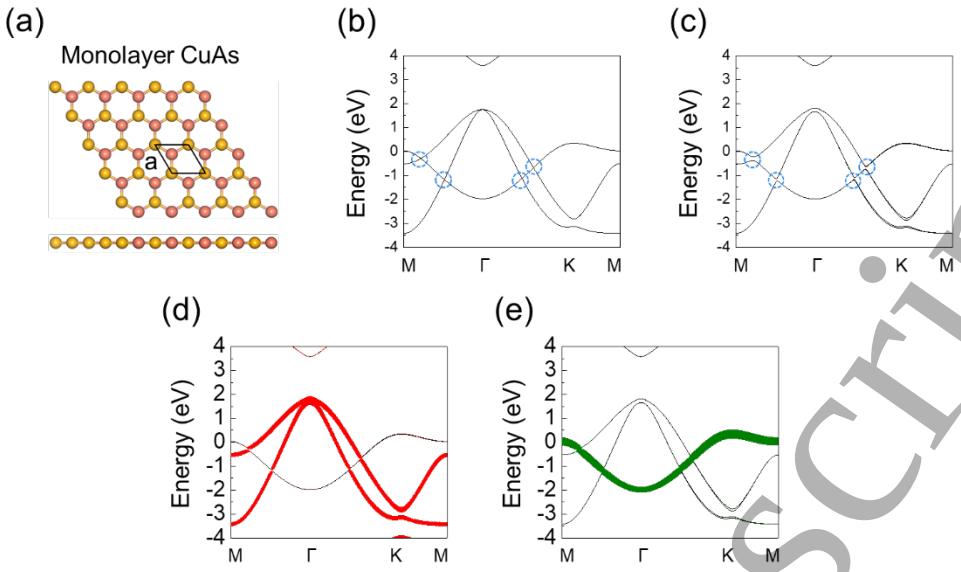

Fig. 4. Calculated electronic structures of free-standing monolayer CuAs. (a) The top view and side view of atomic structure of a monolayer CuAs. The black rhomb marks the unit cell of monolayer CuAs. (b, c) The band structures of a free-standing monolayer CuAs without and with SOC. (d, e) Projected band structure of a free-standing monolayer CuAs with SOC. (d) The two bands marked by red are contributed mainly by in-plane orbitals (As p_x/p_y and Cu d_{xy}/d_{x2-y2}). (e) The band marked by green is contributed mainly by out-of-plane orbitals (As p_z and Cu d_{xz}/d_{yz}).

Moreover, we investigate the intrinsic electronic structure of free-standing monolayer CuAs by DFT calculations. The top view and side view of atomic structure of a monolayer CuAs is shown in Figure 4(a). Monolayer CuAs has a flat structure with a honeycomb lattice. The calculated band structure of freestanding monolayer CuAs without and with the spin–orbital coupling (SOC) effect are shown in Figure 4(b) and (c), respectively. In Figure 4(b), four crossings of the three bands imply Dirac nodal line fermions (DNLFs). [24] While considering SOC, a gap opens around the crossings. which can be attributed to the absence of the mirror reflection symmetry in the CuAs plane, which is similar with free-standing monolayer CuSe.

Compared with free-standing CuAs, the band structures of CuAs on Cu(111) changes mainly in two aspects. Firstly, when the monolayer CuAs is grown on Cu (111) substrate, the upward opening band along M–Γ–K direction of the Brillouin zone of free-standing CuAs disappears. To explain this phenomenon, projected band structures for free-standing CuAs is calculated, shown in Figure 4(d, e). The two hole-like bands marked by red in Figure 4(d) are contributed mainly by in-plane

orbitals (As p_x/p_y and Cu d_{xy}/d_{x2-y2}), while the band marked by green in Figure 4(e) is contributed mainly by out-of-plane orbitals (As p_z and Cu d_{xz}/d_{yz}). As a result, the out-of-plane orbitals of CuAs/Cu(111) are coupled by the substrate. Secondly, the Fermi level of monolayer CuAs on Cu (111) substrate is closer to the top of the hole-like bands, while the Fermi level will shift by about 2.0 eV in a freestanding CuAs. The Fermi level shift of monolayer CuAs on Cu (111) substrate should arise from substrate charge transfer[34]. If more electrons could be transferred, the Fermi level will be lifted further and monolayer CuAs will transform into a semiconductor. Other possible methods to transfer electron also includes surface doping of electron donor, like alkali metal atoms. Recently, it was reported that metallic monolayer honeycomb monochalcogenide MX (M = Cu, Ag; X = S, Se, Te) can be effectively tuned to semiconductor or topological insulator.[35] We believe that effect is also valid for CuAs since they have similar structure and composition, and exotic properties induced by other surface dopants and substrates are worth further investigations.

4. **Conclusions**

In summary, we have successfully synthesized high-quality, single-crystalline, monolayer CuAs by a direct arsenication of a Cu(111) substrate at 470 K. Characterizations by LEED, STM, XPS, and DFT calculations elucidated monolayer structure with honeycomb lattice. The ARPES measurements and their agreement with calculations revealed the metallic electronic structure of the monolayer CuAs. Additionally, first-principle calculated band structures of free-standing CuAs demonstrate that the charge transfer from substrate to monolayer CuAs modulates the Fermi level of monolayer CuAs. This work may enrich the family of 2D materials and provide a new candidate for nano-devices in the future.

References

[1] Novoselov K S, Geim A K, Morozov S V, Jiang D, Zhang Y, Dubonos S V, Grigorieva I V and Firsov A A 2004 *Science* **306** 666

[2] Geim A K and Novoselov K S 2007 *Nat. Mater.* **6** 183

[3] Castro Neto A H, Guinea F, Peres N M R, Novoselov K S and Geim A K 2009 *Reviews of Modern Physics* **81** 109
[4] Bae S, Kim H, Lee Y, Xu X, Park J S, Zheng Y, Balakrishnan J, Lei T, Kim H R, Song Y I, Kim Y J, Kim K S, Ozyilmaz B, Ahn J H, Hong B H and Iijima S 2010 *Nat. Nanotechnol.* **5** 574
[5] Das S, Kim M, Lee J-w and Choi W 2014 *Crit. Rev. Solid State Mater. Sci.* **39** 231
[6] Liu T, Tong L, Huang X and Ye L 2019 *Chinese Physics B* **28** 017302
[7] Lu N, Wang L, Li L and Liu M 2017 *Chinese Physics B* **26** 036804
[8] She Y-C, Wei Z, Luo K-W, Li Y, Zhang Y and Zhang W-X 2018 *Chinese Physics B* **27** 060306
[9] Pan Y, Zhang H, Shi D, Sun J, Du S, Liu F and Gao H-j 2009 *Adv. Mater.* **21** 2777
[10] Meng L, Wang Y, Zhang L, Du S, Wu R, Li L, Zhang Y, Li G, Zhou H, Hofer W A and Gao H J 2013 *Nano Lett.* **13** 685
[11] Li L, Lu S Z, Pan J, Qin Z, Wang Y Q, Wang Y, Cao G Y, Du S and Gao H J 2014 *Adv. Mater.* **26** 4820
[12] Mannix A J, Zhou X F, Kiraly B, Wood J D, Alducin D, Myers B D, Liu X, Fisher B L, Santiago U, Guest J R, Yacaman M J, Ponce A, Oganov A R, Hersam M C and Guisinger N P 2015 *Science* **350** 1513
[13] Deng J, Xia B, Ma X, Chen H, Shan H, Zhai X, Li B, Zhao A, Xu Y, Duan W, Zhang S C, Wang B and Hou J G 2018 *Nat. Mater.* **17** 1081
[14] Wang Q H, Kalantar-Zadeh K, Kis A, Coleman J N and Strano M S 2012 *Nat. Nanotechnol.* **7** 699
[15] Li E, Zhang R-Z, Li H, Liu C, Li G, Wang J-O, Qian T, Ding H, Zhang Y-Y, Du S-X, Lin X and Gao H-J 2018 *Chinese Physics B* **27** 086804
[16] Ji F, Ren X, Zheng X, Liu Y, Pang L, Jiang J and Liu S 2016 *Nanoscale* **8** 8696
[17] Chen Y, Ye D, Wu M, Chen H, Zhang L, Shi J and Wang L 2014 *Adv. Mater.* **26** 7019
[18] Ma Y, Liu B, Zhang A, Chen L, Fathi M, Shen C, Abbas A N, Ge M, Mecklenburg M and Zhou C 2015 *ACS Nano* **9** 7383
[19] Sokolikova M S, Sherrell P C, Palczynski P, Bemmer V L and Mattevi C 2019 *Nat. Commun.* **10** 712
[20] Huang B, Clark G, Navarro-Moratalla E, Klein D R, Cheng R, Seyler K L, Zhong D, Schmidgall E, McGuire M A, Cobden D H, Yao W, Xiao D, Jarillo-Herrero P and Xu X 2017 *Nature* **546** 270
[21] Jiang S, Li L, Wang Z, Mak K F and Shan J 2018 *Nat. Nanotechnol.* **13** 549
[22] Qian K, Gao L, Chen X, Li H, Zhang S, Zhang X L, Zhu S, Yan J, Bao D, Cao L, Shi J A, Lu J, Liu C, Wang J, Qian T, Ding H, Gu L, Zhou W, Zhang Y Y, Lin X, Du S, Ouyang M, Pantelides S T and Gao H J 2020 *Adv. Mater.* e1908314
[23] Lin X, Lu J C, Shao Y, Zhang Y Y, Wu X, Pan J B, Gao L, Zhu S Y, Qian K, Zhang Y F, Bao D L, Li L F, Wang Y Q, Liu Z L, Sun J T, Lei T, Liu C, Wang

J O, Ibrahim K, Leonard D N, Zhou W, Guo H M, Wang Y L, Du S X, Pantelides S T and Gao H J 2017 *Nat. Mater.* **16** 717
[24] Gao L, Sun J T, Lu J C, Li H, Qian K, Zhang S, Zhang Y Y, Qian T, Ding H, Lin X, Du S and Gao H J 2018 *Adv. Mater.* **30** 1707055
[25] Kohn W and Sham L J 1965 *Phys. Rev.* **140** 1133
[26] Kresse G and Furthmuller J 1996 *Comput. Mater. Sci.* **6** 15
[27] Kresse G and Furthmuller J 1996 *Phys. Rev. B* **54** 11169
[28] Cococcioni M and de Gironcoli S 2005 *Phys Rev B* **71** 035105
[29] Wu D, Zhang Q and Tao M 2006 *Phys Rev B* **73** 235206
[30] Powell C J 2012 *J. Electron Spectrosc. Relat. Phenom.* **185** 1
[31] Ghosh S C, Biesinger M C, LaPierre R R and Kruse P 2007 *J. Appl. Phys.* **101**
[32] Lu J, Bao D L, Qian K, Zhang S, Chen H, Lin X, Du S X and Gao H J 2017 *ACS Nano* **11** 1689
[33] Tusche C, Meyerheim H L and Kirschner J 2007 *Phys. Rev. Lett.* **99** 026102
[34] Jiang Y, Sun Y Y, Chen M, Wang Y, Li Z, Song C, He K, Wang L, Chen X, Xue Q K, Ma X and Zhang S B 2012 *Phys. Rev. Lett.* **108** 066809
[35] Gao L, Sun J T, Sethi G, Zhang Y Y, Du S and Liu F 2019 *Nanoscale* **11** 22743